Uncertainty-Aware Visual Analysis of Biochemical Reaction Networks

Corinna Vehlow*, Jan Hasenauer†, Andrei Kramer†, Julian Heinrich*,
Nicole Radde†, Frank Allgöwer†, and Daniel Weiskopf*

* VISUS – Visualization Research Center, University of Stuttgart, Germany
† IST – Institute for Systems Theory and Automatic Control, University of Stuttgart, Germany

ABSTRACT

We present a visual analytics system that supports an uncertainty-aware analysis of static and dynamic attributes of biochemical reaction networks (BRNs). These are often described by mathematical models, such as ordinary differential equations (ODEs), which enable the integration of a multitude of different data and data types using parameter estimation. Due to the limited amount of data, parameter estimation does not necessarily yield a single point in parameter space and many attributes of the model remain uncertain. Our system visualizes the model as a graph, where the statistics of the attributes are mapped to the color of edges and vertices. The graph view is combined with several linked views such as lineplots, scatterplots, and correlation matrices, to support the identification of uncertainties and the analysis of their mutual dependencies as well as their time dependencies. To assess the utility of the individual visualization approaches and multiple linked views, a qualitative user study with domain experts was performed. We found that all users were able to process analysis tasks using our system.

Keywords: Network visualization, uncertainty visualization, biochemical reaction networks

Index Terms: H.5.m [Information Systems]: Information Interfaces and Presentation—Miscellaneous; J.3 [Computer Applications]: Life and Medical Sciences—Biology and genetics;

1 INTRODUCTION

Most properties of intracellular biological systems arise from the complex interaction of biochemical species (e.g., genes and proteins). The interaction structure and the underlying interaction mechanisms can be described using BRNs. BRNs can be used to collect the knowledge available about the system of interest. It has been realized that models of biochemical reaction networks are powerful tools and may help us gain a holistic understanding of specific cell functions or diseases [20]. Therefore, models of BRNs have become state-of-the-art tools used in academia and industry alike. There are different reasons for analyzing BRNs, such as the detection of potential drug targets to treat a certain disease. This model-based detection reduces the need for large screening studies and enables a faster and cheaper drug development process [30].

Biological systems of this kind can be described by mathematical models, such as ODEs. To allow the reliable prediction of drug targets, a multitude of different data and data types has to be incorporated into the ODE model using parameter estimation. As the models are often high-dimensional and contain many unknown parameters, parameter estimation does in general not provide a unique result, especially considering the limited amount of data. One common way to deal with that property is to obtain a sample of potential parameters that provide a reasonable fit of the data [8, 21, 37]. The analysis of the model uncertainties, encoded within these samples, is essential to draw grounded conclusions about the systems' behavior. Various tools are available to simulate and visualize BRN models but hardly any tools exist that would support the visual analysis of uncertainties in BRN models.

In this work, we present a visual analytics system that enables the user to perform an in-depth study of uncertain BRNs. We focus on BRN models by ODEs and parameters estimated using Bayesian estimation approaches. Bayesian estimation directly provides the statistics of network attributes, including the static model parameters and the dynamic concentrations and fluxes. Our visual analytics system visualizes attribute uncertainties and their time-dependence directly within the graph view and within different linked views. The biological networks are displayed as node-link diagrams and attributes are mapped to the color of the respective elements (edges or nodes). The user can explore the BRN model with linked views, such as lineplots, scatterplots, and correlation matrices. The utility of the individual visualization methods as well as the linking is assessed with a qualitative user study with 10 domain experts.

2 APPLICATION BACKGROUND

In this section, we briefly review the basics of BRNs. These include ODE-based modeling, Bayesian parameter estimation, and uncertainty analysis (see Figure 1). Based upon this, we derive the analysis and visualization requirements.

2.1 Biochemical Reaction Networks

Biochemical reaction networks consist of chemical species $(X_1, X_2, \ldots, X_{n_x})$ and reactions $(R_1, R_2, \ldots, R_{n_r})$. A chemical species is an ensemble of chemically identical molecular entities, such as proteins and metabolites, whereas a process that results in the interconversion of chemical species is referred to as chemical reaction [26], e.g., phosphorylation.

Chemical reactions are defined via lists of reactants (r) and products (p), and can be written as:

$$R_j: \quad \sum_{i=1}^{n_x} s_{ij}^{(r)} X_i \rightarrow \sum_{i=1}^{n_x} s_{ij}^{(p)} X_i, \quad j = 1, \ldots, n_r,$$

where, $s_{ij}^{(r)}$ $(s_{ij}^{(p)}) \in \mathbb{N}_0$ is the stoichiometric coefficient of species i in reaction j. This coefficient denotes the number of molecules consumed (produced) when the reaction takes place [20].

BRNs can be interpreted as a directed graph where vertices represent species X_i and edges represent reactions R_j. The vertex and edge structure is coded in the stoichiometric matrix S. Besides regular directed edges that represent interconversions between species, directed hyper-edges from a species to a reaction resulting from regulatory interactions may exist. If species X_i influences the rate of reaction R_j without being consumed, it is a modifier of R_j.

*E-mail: {vehlow, heinrich, weiskopf}@visus.uni-stuttgart.de
†E-mail: {hasenauer, kramer, radde, allgower}@ist.uni-stuttgart.de

IEEE Symposium on Biological Data Visualization 2012
October 14 - 15, Seattle, Washington, USA
978-1-4673-4730-3/12/$31.00 ©2012 IEEE

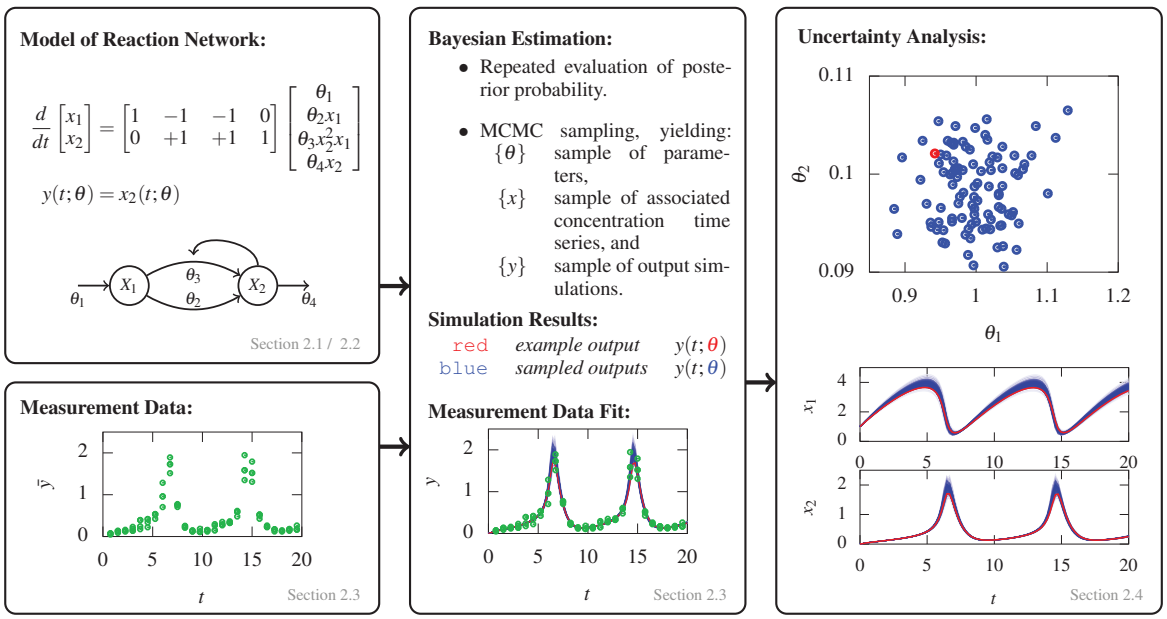

Figure 1: Workflow of model development, including the derivation of a parametric ODE model and the data collection (left), the parameter estimation (middle), and the uncertainty analysis (right).

2.2 Ordinary Differential Equation Models of Biochemical Reaction Networks

In the following, the dynamics of the BRNs are modeled using ODEs. ODE models of BRNs are commonly written as:

$$\dot{x} = Sv(x,\theta), \quad x(0) = x_0(\theta), \tag{1}$$

in which $x(t)$ is the state at time t, with x_i being the concentration of the chemical species X_i. Furthermore, $x_0(\theta)$ is the parameter dependent initial condition, $S = \{S_{ij} = s_{ij}^{(\mathrm{p})} - s_{ij}^{(\mathrm{r})}\}$ is the stoichiometric matrix, $v(x,\theta)$ is the flux vector, and θ is the parameter vector. While the state $x(t)$ provides information about the current conditions, the flux $v(x,\theta)$ determines the change of the state with time t. The flux $v_j(x,\theta)$ is often modeled using mass action kinetics [20], yielding

$$v_j(x,\theta) = \theta_j \prod_{i=1}^{n_\mathrm{x}} x_j^{s_{ij}^{(\mathrm{r})}}, \quad j = 1,\ldots,n_\mathrm{r}. \tag{2}$$

In this context, parameters θ_j are reaction rate coefficients.

In a graph representation, the time-dependent states $x_i(t)$ are attributes of the vertices. The edges have two attributes: the time-dependent fluxes $v_j(x(t),\theta)$ and the parameters θ_j.

While the ODE framework is highly flexible and allows for the description of many metabolic, signal transduction, and gene regulation processes, it suffers like most other modeling approaches from one major problem: due to experimental constraints, the parameters θ_j cannot be measured directly, but have to be estimated.

2.3 Bayesian Parameter Estimation

To estimate the parameters θ_j, measurement data are collected. The measured quantities $y(t) = h(x,\theta)$ (also called outputs), typically are individual states variables ($h_i(x,\theta) = x_j$) or sums of states ($h_i(x,\theta) = x_{j_1} + x_{j_2}$). As the measurements are affected by noise, the available data are: $\mathscr{D} = \{(\bar{y}(t_k) = y(t_k) + \varepsilon(t_k), t_k)\}_{k=1}^{n_t}$ in which t_k, $\bar{y}(t_k)$, and $\varepsilon(t_k)$ denote the time at which the measurement was performed, the noise-corrupted output, and the noise, respectively.

Given the data $\mathscr{D}$, the parameters are reconstructed. Therefore, Bayesian parameter estimation [21, 36] can be used, relying on

$$p(\theta|\mathscr{D}) \propto p(\mathscr{D}|\theta)p(\theta). \tag{3}$$

Here $p(\theta|\mathscr{D})$ is the posterior probability of a parameter vector θ given the data $\mathscr{D}$, which is proportional to the product of the conditional probability $p(\mathscr{D}|\theta)$ and prior knowledge $p(\theta)$.

2.4 Uncertainties of Parameters, Fluxes, and States

Typically, the parameters θ_j cannot be estimated uniquely but remain uncertain. This uncertainty is encoded in the shape of the posterior probability $p(\mathscr{D}|\theta)$. As the parameter vector θ is often high-dimensional, $n_\theta \gg 1$, the analysis of $p(\mathscr{D}|\theta)$ is challenging.

To analyze the uncertainty, a sample $\{\theta^{(l)}\}_{l=1}^{n_\mathrm{s}}$ from $p(\mathscr{D}|\theta)$ is generated, using Markov chain Monte Carlo (MCMC) sampling [25]. Associated to this parameter sample, we have a flux sample $\{v^{(l)}(t)\}_{l=1}^{n_\mathrm{s}}$ and a state sample $\{x^{(l)}(t)\}_{l=1}^{n_\mathrm{s}}$. The individual sample members are flux trajectories $v^{(l)}(t) := v(x^{(l)}(t),\theta^{(l)})$ and state trajectories $x^{(l)}(t) := x(t;\theta^{(l)})$, respectively, obtained for simulating model (1) with parameter $\theta^{(l)}$. These samples $\{\theta^{(l)}\}_{l=1}^{n_\mathrm{s}}$, $\{v^{(l)}(t)\}_{l=1}^{n_\mathrm{s}}$, and $\{x^{(l)}(t)\}_{l=1}^{n_\mathrm{s}}$ carry the statistical properties of $p(\mathscr{D}|\theta)$ as well as its image in flux and concentration space. Hence, the samples can be used to gain insight into the parameter and prediction uncertainties.

2.5 Goals of the Uncertainty Analysis and Requirements

Understanding the uncertainties is key to ensure good comprehension of the model and its limitations, and to allow the selection of future experiments. Unfortunately, an in-depth analysis of the uncertainty is ambitious because it has a multitude of different dimensions. In particular, static and dynamic attributes are present, and hidden dependencies between attributes of different vertices and edges are of interest.

So far, domain experts mainly used tables, scatterplots, and lineplots of existing systems individually to investigate parameter, flux,

and concentration samples. In doing so, it is hard to detect complex patterns within the data as it is not possible to obtain a detailed view of the distributions. To achieve this, it is necessary to provide linked visualizations for the analysis of individual attributes of the BRN model. In particular, exploration approaches are essential ingredients, as they allow the user to subsequently focus on the following Analysis Tasks:

1. assessment of relatively high uncertainties.
2. localization of uncertainties hubs.
3. analysis of time-dependence of fluxes and concentrations and their time-dependent uncertainties.
4. localization of hubs involved in fast or slow process dynamics.
5. characterization of correlations between attributes, e.g., between parameters, fluxes, or concentrations.

In order to help the target users, who are in our case systems biologists and biomathematicians, to perform the above mentioned analysis tasks, it is essential to develop a system that includes views onto the data whose functionality matches the expectations of the users. As argued by Plaisant, it is therefore necessary "to study the design context for visualization tools including tasks, work environments and current work practice" [22]. Our visual analytics system was developed in a participatory design process using evolutionary prototypes [6]. Concerning the seven evaluation scenarios by Lam et al. [22], studying the target users using observations and interviews falls into the category "Understanding Environments and Work Practices". Besides conducting an initial interview for a first requirements analysis, we involved two target users in all phases of the design process to refine requirements, to evaluate concrete ideas about views, and to select the best from different alternatives. During the entire design cycle of about six months, meetings with the two collaborators were held regularly, typically on a biweekly basis. Feedback from the target users concerning possible views and interactions, gained during these meetings, could therefore directly be incorporated into the development process.

3 Related Work

Biochemical reaction networks are usually displayed as node-link diagrams, where chemical species are represented as vertex glyphs and reactions by arrows between them. The vertices and edges of a graph may be provided with domain-specific attributes, such as parameters, fluxes, and concentrations within BRNs, that describe properties of objects or relations. These can be mapped to visual attributes of vertices, such as their size, shape, color, or brightness, and visual attributes of edges, such as their length, thickness, color, or brightness [15].

Where the structure of BRNs is fixed, attributes attached to vertices (concentrations) and edges (fluxes) can change. There are three common visualization methods used to overlay the evolution of multi-dimensional information onto graphs [7]: animation, small multiples [31], and complex glyphs, such as small charts embedded into the graph.

Although there is a large number of visualization tools for biochemical reaction networks, only few of them support the visualization of dynamic node attributes describing experimental data values. Tools, such as GENeVis [35], VANTED [18], Cerebral [5], Pathline [27], and the Pathway Tools software [19], visualize gene regulatory networks and related gene expression values at specific time steps. While GENeVis and VANTED make use of small charts embedded into the vertices, Cerebral and Pathline use small multiple views of the graph or line charts of the time-series data. These approaches work fine for their applications due to the manageable number of time steps but do not scale well for much longer time series. In contrast, the Pathway Tools software visualizes attribute dynamics using animation instead of a static representation.

Besides the visual analysis of time dependancies of attributes of BRNs, particularly the analysis of attribute uncertainties is of interest for a reliable assessment of potential drug targets. Unfortunately, hardly any tools exist that visualize these uncertainties. Tools, such as COPASI [14] or CellDesigner [12], support the simulation of BRN models and visualization of model predictions. While these tools are suitable given that we are interested in just one parameter value, they fail to provide visualizations of the prediction uncertainties. Finally, available tools do not support a visual exploration of network and prediction uncertainties.

The quantification and visualization of uncertainties within experimental or simulated data has been recognized as one of the most important issues in scientific visualization [16]. Often, uncertainties originate during data acquisition and due to limited amounts of data. In our application, information about the model uncertainties are assessed during parameter estimation. Uncertainties can be quantitatively described by statistical properties like probability, error, percentage, and standard deviation. These values can be directly visualized using one of the possible approaches: adding glyphs or geometry to the rendered scene, modifying geometry, modifying attributes of the geometry, animation, or addressing other human senses [28]. A common approach is the modification of geometry using visual attributes, like color, size, position, transparency and so on, or the plotting of discrete data points as glyphs (e.g., box plots or quartile plots) with specific visual attributes.

While there is extensive research on visualization of uncertainties of flow fields and surface representations [13, 17], only little work has been done on visualizing uncertainties within graphs, i.e., the uncertainties of relations or attributes of the graph. Collins et al. [10] visualized uncertainties of translations using lattice graphs that show multiple linear paths for a translation. Cesario et al. [9] visualized uncertainties of multiple static node attributes using a spatial layout and multiple linked views such as bullseye, comparative column, scatterplot, and parallel coordinates. Their approach was particularly designed to compare two static graphs and their attributes. CandidTree was developed by Lee et al. [23] to visualize structural uncertainties. To the best of our knowledge, there exists no tool that visualizes attribute uncertainties directly within the graph, e.g., by mapping them to visual attributes of nodes or edges.

4 Visual Analytics System

To analyze the estimation quality of static parameters (θ), dynamic fluxes (v), and dynamic concentrations (x, also referred to as states) of the system model, it is necessary to get an overview of the summary statistics of samples, like mean and standard deviation. These can be mapped to visual attributes of the graph (see Figure 2). At the same time, the distribution of values within the samples needs to be investigated and should be visually available to the user. Hence, our system uses multiple linked views to visualize summary statistics and distributions of values within samples, the dynamic change of samples and correlations between sample members or time courses. We use brushing and linking to show the correspondence of elements in different views. If the selection within one view changes by brushing, the respective elements within all views are first highlighted by short flashing before they stay highlighted.

In the following sections, we present different methods that can be used to analyze data uncertainties, dynamics, and correlations to solve the aforementioned Analysis Tasks (Section 2.5). A small case study used for the qualitative user study is shown in Figure 4.

4.1 Visualization of Attribute Samples

MCMC sampling does not only provide a sample of the parameters $\{\theta^{(l)}\}_{l=1}^{n_s}$, but also the fluxes $\{v^{(l)}(t)\}_{l=1}^{n_s}$ and reactant concentrations $\{x^{(l)}(t)\}_{l=1}^{n_s}$. Before the mean and standard deviation of a

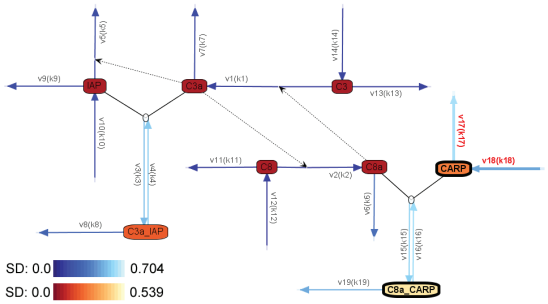

Figure 2: Graph of the *Caspase Cascade Eissing* model for apoptosis. The colors of the edges elucidate the uncertainty of the parameters of the respective reactions (θ_j) and the colors of the vertices illustrate the uncertainty of the concentrations of the respective compounds at the steady state. There is a strong correlation between the parameter samples $\{\theta_{17}{}^{(l)}\}_{l=1}^{n_s}$ and $\{\theta_{18}{}^{(l)}\}_{l=1}^{n_s}$ (respective edges for R_{17} and R_{18} are selected and thus highlighted). The two species whose concentrations have been predicted with high uncertainty (CARP and C8a_CARP) are selected and highlighted. See time courses for these concentrations in Figure 3.

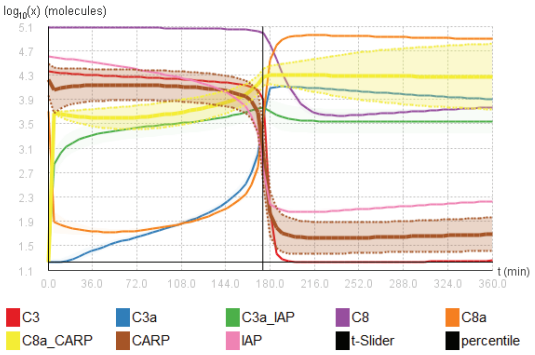

Figure 3: Lineplot of the evolution of concentrations ($x_i(t)$) within the *Caspase Cascade Eissing* model. Lines are surrounded by semitransparent areas representing the uncertainty. The time course of the concentrations for the selected compounds CARP and C8a_CARP are highlighted, i.e., the line width is increased and the area around the line is less transparent than for the other time courses. These are the compounds that have been predicted with the highest uncertainty. The plot illustrates that for many compounds the concentration changes drastically around t=175 min and the time courses converge towards the steady state. The thin vertical black line indicates the currently selected time point (t=175 min).

sample are calculated, the values are transformed using the logarithm to the base 10 ($\log_{10}$). For fluxes and concentrations, we first compute the 5-percentile, which we later use as a threshold to cut off small values we do not want to differentiate.

The standard deviation of a sample is a measure of uncertainty of this attribute. Due to the log-transformation the computed uncertainties are the relative uncertainties of the associated (non-transformed) attributes. To support the user in Analysis Tasks 1 and 2, the statistical variables mean and standard deviation are visualized by modifying the color of the respective objects. Ware and Beatty [34] stated that color scales based on an approximation to the physical spectrum are effective to convey metric information. The statistical values can be mapped to the color of edges (for θ_j and $v_j(x(t),\theta)$) and vertices (for $x_i(t)$) either individually or in combination. For edges, only one of the two attributes (θ_j or $v_j(x(t),\theta)$) can be visualized at a time.

The mean of an attribute sample can be mapped to color using continuous multi-hue colormaps that map the mean values linearly to a range of hues with monotonously changing brightness. Before this color-mapping, a thresholding of mean values based on the aforementioned 5-percentile is applied. The target users chose a subset of different multi-hue colormaps that are available within the system. Using these colormaps, users can easily identify relatively high and small values, which is essential as the target users noted that it is mainly of interest to analyze the differences of mean values instead of the absolute value.

The uncertainty of an attribute sample is mapped to the saturation of the color. If only uncertainty is visualized, the standard deviation is mapped to color using a univariate single-hue colormap, where the standard deviation determines the saturation of the color. Although it is hard to differentiate hue and saturation simultaneously, we decided to incorporate a bivariate multi-hue colormap to allow users to visualize mean and standard deviation simultaneously.

For parameters θ_j, an overview of all mean values and standard deviations is available within a table. The cells of the table are colored using the selected color maps for edges for mean values and standard deviations, respectively. Hence, the lowest and highest mean values and standard deviations for the parameters of the system can be identified at a glance, which fulfills Analysis Task 1. Relatively high uncertainties are of no consequence for the systems' behavior, if the parameter value itself is relatively low. In contrast, for a high parameter θ_j high uncertainties predominate, i.e., that the concentration x_i of the species X_i involved in the respective reaction R_j, as well as the flux v_j of R_j are likely to be estimated with uncertainty, too.

To investigate the distribution of values within parameter samples $\{\theta^{(l)}\}_{l=1}^{n_s}$, the user can open a *histogram view* including the histograms for a set of selected parameters (edges). The histograms are computed with the same bin width and are thus comparable.

4.2 Visualization of the Attribute Dynamics

As introduced in Section 2.2, BRNs are dynamic and so are concentrations and fluxes. For the analysis of the systems' behavior, particularly the comparison of different time series for various fluxes $v_j(x(t),\theta)$ or concentrations $x_i(t)$ is of interest. Furthermore, system biologists want to analyze the change of uncertainty over time and whether a steady state was reached for all components. As mentioned in Section 3, dynamic graphs can be visualized in three ways: using small multiples, animation, or small embedded charts. The use of small embedded charts, i.e., the visual stacking of charts within the graph, lacks the aforementioned data Analysis Tasks, particularly the comparison of time series. Using this approach, each time series of a concentration or flux would be plotted within an individual chart within the respective node or adjacent to the respective edge. It would be hard to compare different time series that are plotted apart from each other and furthermore do not share a common reference point. Furthermore, for long time series data, the embedded charts would become too large, leading either to occlusion of objects or a graph layout exceeding the available screen space. Also the approach of small multiples does not scale for the large number of time steps (about 100 time steps) the simulations comprise, due to the partitioning of available display space. Animation poses a natural way to convey dynamic data as it is consistent with the users expectation. At the same time, its effectiveness is limited due to perceptual and cognitive limitations in the processing of changing visual presentations [32]. Therefore, changes within the graph should be highlighted [33]. We incorporated animation within our system mainly to support the user in getting an overview of when something changes drastically and in identifying hubs within the network, where changes appear in a time in-

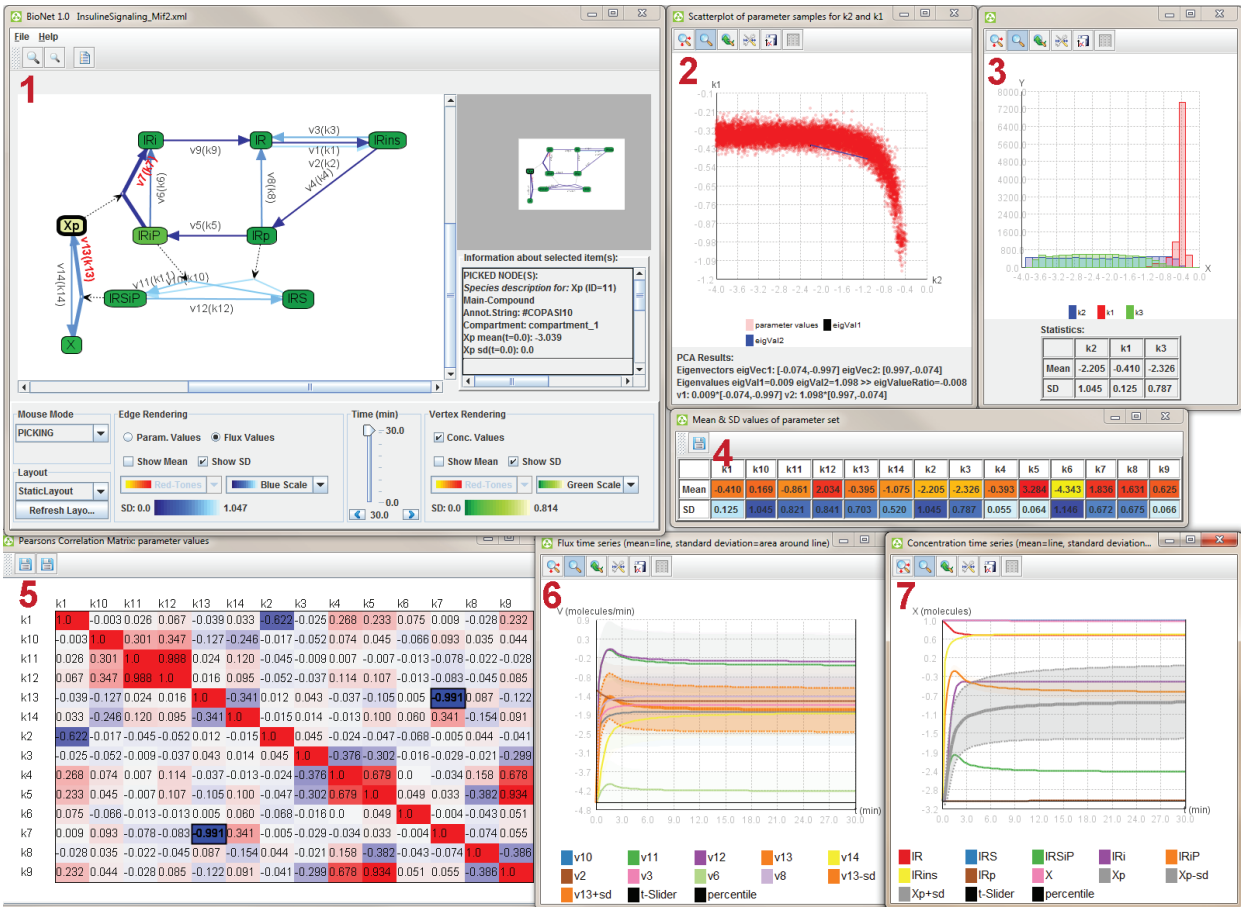

Figure 4: (1): *Insulin signaling model* to illustrate the use of our visual analytics system. Edges and vertices are colored based on the standard deviation at the steady state (t=30 min) of flux samples $\{v^{(l)}(t)\}_{l=1}^{n_s}$ and concentrations $\{x^{(l)}(t)\}_{l=1}^{n_s}$, respectively. The time courses of fluxes and concentrations can be analyzed within lineplots (see (6) and (7)), where within (6) the lines for all fluxes that have been predicted reliably are hidden to reduce clutter. The table of mean values and standard deviations for the static parameter samples $\{\theta^{(l)}\}_{l=1}^{n_s}$ (see (4)) shows that there are several uncertain parameters. Merely the samples of four parameters k_1, k_4, k_5 and k_9 possess standard deviations close to zero. The histogram (see (3)) allows for the detailed study of the distribution of individual parameters and shows here that k_1 is rather certain whereas k_2 and k_3 are uncertain. The Pearson correlation matrix (see (5)) reveals a strong anti-correlation of k_7 and k_{13} (selected cell within the matrix and hence respective edges within the graph view (1) and lines within the line plot (6) are highlighted). Furthermore, there is a slight anti-correlation between k_1 and k_2, which is confirmed by the scatterplot for the respective two samples (see (2)). In (1) and (7), we see that Xp is the species with the highest uncertainty. The analysis of this system model was captured and summarized within a video (see additional material).

terval of interest (Analysis Task 4). Thereby, the mean value or standard deviation of a sample $\{v^{(l)}(t)\}_{l=1}^{n_s}$ ($\{x^{(l)}(t)\}_{l=1}^{n_s}$) for the selected time step t_k is mapped to the color of the respective edge (vertex). The user can navigate through time either rapidly with the help of a slider or stepwise using the forward or backward button. It is also possible to start an automatic run through time by keeping one of the buttons pressed. During the automatic animation, drastic changes of the mean or standard deviation of the samples $\{v^{(l)}(t)\}_{l=1}^{n_s}$ ($\{x^{(l)}(t)\}_{l=1}^{n_s}$) are automatically detected and respective edges (vertices) are briefly highlighted within the graph.

Animation supports the user in getting an overview about the changes but does not allow for a detailed analysis and comparison of all time series for fluxes or concentrations (Analysis Task 3). Therefore, we decided to visualize the mean values and standard deviations of $\{v^{(l)}(t)\}_{l=1}^{n_s}$ ($\{x^{(l)}(t)\}_{l=1}^{n_s}$) in separate lineplots, where each line within the plot corresponds to the mean time course of a specific flux v_j (concentration x_i). To visualize the uncertainty of the flux (concentration) over time, we decided to frame each line by a semitransparent area indicating the uncertainty, instead of using common glyphs like box plots or quartile plots. The lines are colored based on a color map created with ColorBrewer [3]. An additional vertical line within the plot indicates the current time step and is updated during animation. The *lineplot view* is linked to the *graph display* in a way that the respective lines and areas representing the uncertainty for selected edges (vertices) are highlighted within the lineplot and vice versa (see Figures 3 and 4). Time courses can also be highlighted by hovering over the lines. With increasing size of the BRN and thus number of reactions and species, the lineplots for fluxes and concentrations become cluttered. Furthermore, it is difficult to distinguish more than approximately 10 colors and thus to allocate time series with respective reactions (species). Therefore, lines can be faded out instead of just highlighting selected elements to focus on fluxes (concentrations) of interest.

4.3 Visualization of Correlations Between Attributes

Another Analysis Task (Task 5) defined by the target users is the identification of correlations between uncertainties within the system. Often, uncertainty in one attribute comes along with uncer-

tainty in some other attributes. Besides, the values of two attributes, e.g., two parameters in $\{\theta^{(l)}\}_{l=1}^{n_s}$, might be correlated. Two different matrix views are available that can be used to investigate dependencies of or correlation between different dimensions of the parameter sample $\{\theta^{(l)}\}_{l=1}^{n_s}$: an eigenvalue-ratio-matrix and a correlation matrix. Where the former is based on principal component analysis (PCA), the correlation matrix includes Pearson's correlation coefficients for all pairwise combinations of parameter samples. For fluxes (concentrations), the correlation matrix displays the pairwise Pearson's correlation between time courses of either mean values or standard deviations instead of sample members. The cells within this matrix include the numerical values and are colored with respect to the sign and absolute value of the ratio (see (5) in Figure 4). In particular, we used a classic cool-warm color map that maps negative values to blue and positive values to red, where the smaller the absolute value, the less saturated is the color.

Similar to the *lineplot views*, also the *matrix views* are linked to the *graph display*. Hence, if a cell within the matrix is selected, the two respective elements within the graph as well as the respective lines within the *lineplot view* are highlighted. Vice versa, if the user selects two edges (vertices) within the graph, the respective cell within the *matrix view* is highlighted.

While the matrices can be used to obtain an overview of occurring correlations within the system, scatterplots can be used to gain further insights into the kind of correlation and distribution of values in the sample (see (2) in Figure 4). Therefore, it is possible to open a scatterplot of the samples of two elements ($\{\theta^{(l)}\}_{l=1}^{n_s}$, $\{v^{(l)}(t)\}_{l=1}^{n_s}$, $\{x^{(l)}(t)\}_{l=1}^{n_s}$), directly selected within the graph or indirectly by selecting a matrix cell. For fluxes and concentrations, only samples for the currently selected time point t_k are visualized within the scatterplot. The scatterplot view also shows the results of the PCA, performed on the two samples, including the eigenvectors and eigenvalues.

4.4 Implementation

The visual analytics approach (see Figure 4 and movies within the supplemental material) is implemented in Java. For the network visualization, we make use of the Java Universal Network/Graph Framework Version 2.0.1 [1]. As basis for the diverse plots, including lineplots, histograms and scatterplots, we use the package JMathPlot of the Java library JMathTools [2].

BRNs are stored using the Systems Biology Markup Language (SBML) [4], a widely established interchange format, used to describe qualitative and quantitative models.

5 Qualitative User Study with Domain Experts

After the participatory design process of our visual analytics system, we performed a qualitative user study with a larger group of experts from the respective domain, i.e., potential target users. Due to quality concerns, Perer and Shneiderman recommended the use of domain experts for evaluations [29]. Concerning the seven evaluation scenarios by Lam et al. [22], our study falls under the category "Evaluating User Experience". Such evaluations are used to "study people's subjective feedback and opinions", i.e., to analyze the subjective preferences concerning views and features of the tool, and to investigate "to what extent visualization supports the intended tasks". The intended Analysis Tasks were described in Section 2.5, including tasks related to uncertainty, time dependance, and correlations. As measurements of usability we used different qualitative data including the participants comments, investigators' observations as well as the results of the evaluation survey [11, 22]. An evaluator took notes of interesting behavior while the participants interacted with the tool. Furthermore, the participants were asked to fill out a laboratory questionary in a 5-point Likert scale.

5.1 Participants and Equipment

The participants of the qualitative user study work in the field of systems biology and were familiar with BRN models as well as the process of parameter estimation. The group of participants did not include the collaborators that were involved in the formative design process and consisted of 10 people (7 male, 3 female), six of whom have already received the M.Sc. degree or higher while the remaining are still working toward their M.Sc.degree. Six participants are working with system models of biological networks and the problem of parameter estimation and related uncertainties on a regular basis during their work (10-40 hours per week). Although the majority of the participants did not have extensive experience with visualization tools, they were at least familiar with common types of plots, such as lineplots and scatterplots. These information could be retrieved based on the questionaries the participants were asked to fill in during the informing session (see Section 5.2).

We used a desktop computer running Windows 7, a camcorder, two 21" displays, and standard devices such as keyboard and mouse. As the tool comprises several visualizations that can be opened within separate windows, we decided to provide two displays. In this way, the participants were able to look at several views at the same time, without squeezing the views too much.

5.2 Study Procedure

In the beginning, the participants were informed about the procedure as well as the aim and the voluntary nature of the experiment. During the informing session, each participant was asked to fill in a questionary about their educational background and familiarity concerning certain visualizations. Furthermore, two vision tests were performed, one Snellen chart test to measure visual acuity and the Ishihara test for color blindness. As a result, we found that all participants had normal or corrected-to-normal vision, except for one, who reported to have dyschromatopsia. This participant naturally made less use of color maps but could still work with our system and accomplish the analysis tasks.

During the introductory session, the participants were given time to become familiar with the tool, its capabilities, possible views, and interactions. Here, they were given a small example data set and a manual describing the tool. Furthermore, they were encouraged to ask the experimenter if they were unsure concerning the interaction with, or content of, views. In the next step, the list of analysis tasks (see supplemental material) was handed over to the participant. Before the users had to analyze the two given system models, they were asked to do some further exercise analyzing the example data set. The nine analysis tasks have been elaborated together with the target users from the design process to meet their analysis requirements for biological system models. The tasks were grouped into investigative tasks for parameters, fluxes, and concentrations. They aimed at the identification of relatively high uncertainties within the system as well as the change of uncertainties of fluxes and concentrations over time. Another group of analysis tasks aimed at the identification of correlations between attributes of the same type, i.e., between parameters, fluxes, or concentrations, but also between fluxes and states. For the latter, correlations during the steady state were of particular interest. The participants were also asked to analyze the time course itself, i.e., they were asked to identify time intervals of drastic changes, and fluxes as well as concentrations that were subject to strong changes.

Each participant was asked to accomplish these tasks for two different data sets. The participants were asked to "think aloud" [24] and communicate their thoughts as well as the answers to the analysis tasks during the experiment. The aim of using this technique was to understand how they used and interpreted the different available data views to process the analysis tasks and gain insight into different data aspects. During the experiment session, the participants were observed by the experimenter, who made notes about

the users' behavior, applied strategies to solve the tasks, used views, predominant interactions, etc. Furthermore, their interactions and comments were recorded by a camcorder, to complement the qualitative analysis of the participants' behavior.

After the experiment was finished, the participants were asked to fill in a questionaire to evaluate the study procedure and the visual analytics approach using a 5-point Likert scale (see supplemental material). In particular, they were asked to rate the usefulness of all single views, possible visualizations of attribute uncertainties and dynamics as well as included features, like brushing and linking. The whole study procedure took on average 2 hours per participant.

5.3 Study Results

5.3.1 User Performance

Before we started the user study with the 10 participants, one of the target users from the design process was passing through the whole process himself. He analyzed the same two data sets as the participants of the study, including a system model for insulin signaling and apoptosis. Since he was involved in the design process, his feedback was not included in the evaluations in Sections 5.3.2 and 5.3.3. However, the results of his data analysis could be used as "ground truth" to assess the correctness of the participants answers to the analysis tasks. As a result, all participants were able to accomplish the nine tasks and analyze the data.

5.3.2 Task Specific View Preferences

The aim of the analysis procedure was to investigate user-specific preferences concerning views and features they used to analyze certain aspects of the data, such as uncertainty, dynamics, and correlations. We observed that the participants had some preferences in common, when accomplishing certain tasks.

When searching for the most uncertain parameters of the system, most participants (7 out of 10) directly reverted to the table of mean values and standard deviations. At the latest, when they had to analyze the local distribution of uncertainties within the network, they used the color mapping of parameter uncertainties onto edges. Using the table only, it was not possible for them to find out whether there were subnetworks that were predominantly uncertain or if uncertainties were equally distributed within the network.

To analyze the time course of flux and concentration values and related uncertainties, most participants relied on the lineplots, where half of them used animation as a first tool to obtain an overview of where and when changes occurred within the network. However, except for one, all of them used the lineplot to determine time intervals of and elements affected by strong changes. Many of them used the "vertical timeline" within the lineplot, which indicates the selected time step and moves when sliding through time in the main interface, to determine the intervals exactly. The study confirmed that users prefer static displays over animation, when they have to analyze time courses. This is not much of a surprise, as many studies before showed that static views outperform animations, when visualizing dynamic data.

Almost all participants took advantage of the brushing and linking between the views to allocate lines and edges/vertices, where some preferred to select elements within the graph display and others preferred to select lines within the lineplot. Two participants used the legend of the lineplot only to allocate elements; these were participants that did not make use of the available screen space to arrange the views next to each other. It was observed that in total three participants tended to maximize all views or at least to arrange them on top of each other. To take advantage of the linking of views and to simplify the allocation of elements, it might be reasonable to embed the views within one window or to support a docking of windows. The latter might thereby be more useful, as we do not want to show all available views at the same time, but a subset of views that helps us accomplish a specific analysis task.

When trying to analyze correlations between attribute samples, the participants mostly looked at the correlation matrix to identify strong correlations and anti-correlations. To find out whether two specific parameters were correlated, they looked for the respective cell of the matrix or selected the respective edges in the graph to highlight the cell. The other way round, they selected a cell to identify the corresponding two edges within the graph. Only 3 participants looked at the scatterplot of two correlated parameter samples to investigate the kind of correlation and shape of the point cloud.

5.3.3 Subjective Preferences

The participants were asked to evaluate the usefulness of the single views and features of the tool for the accomplishment of the analysis tasks. To do so, they were given a 5-point Likert scale from full agreement (1 = absolutely useful) to full disagreement (0 = not useful at all).

On average, they judged the correlation matrix as most useful view (0.925), followed by the lineplot (0.9), graph view (0.85), and scatterplot (0.813). The histogram was used by only two participants and was therefore evaluated only by these. The participants preferred the mapping of the standard deviation to color (0.825) over the combined mapping of mean value and standard deviation (0.575). We were not surprised that users prefer to map only one attribute to color, as most people have difficulties to differentiate hues and saturations at the same time. However, this does not pose a problem, as users are usually interested in only one of the two statistical measures.

Besides the mapping of uncertainty to color, also the visualization of the standard deviation over time as half-transparent band around the line was rated as very useful (0.944). Also brushing and linking (0.95) and the short flashing of components (0.825) to attract the users attention to these component were valued to be useful. To analyze the time course of mean values and standard deviations, participants preferred the lineplot (0.972) over the sliding through time (0.85) and animated navigation (0.75). This again confirms that static views outperform animations.

6 Conclusion and Outlook

We have developed a visual analytics system, supporting the analysis of BRNs and their properties, in particular parameters, fluxes, and concentrations. These BRNs can be modeled by ODE systems to answer biological questions, e.g., which components trigger certain responses or symptoms. These biological questions can only be answered correctly, if the parameters affecting the kinetics and thus fluxes and finally concentrations of chemical species are known at a minimum degree of certainty. In our application, the information about the parameter and model uncertainty were extracted using Bayesian parameter estimation. Nevertheless, our visual analytics system could directly be extended to make use of other methods, for instance, those presented by Brännmark et al. [8].

The visual analytics approach allows users to identify components and subnetworks of the model of relative high uncertainty. The tool offers several different views onto the data, its statistics and dynamics. These views are linked with each other to simplify the allocation of elements within the different views. Based on the knowledge about uncertain attributes, the user can select and perform additional experiments to reduce uncertainties of specific areas or components of the system.

During the user study with domain experts, we observed that many users were overwhelmed by the number of available views. Most of the participants were used to work with simple visualizations, such as tables and lineplots. Therefore, many participants first of all made use of these views and only familiarized themselves with other available views and color mappings in the course of the study. For test purposes, one of the two collaborators also

passed through the same study procedure but outside of the evaluation. Compared to the 10 participants, it was much easier for him to make use of the available views. This indicates that a longer phase of learning than the participants had during the study is necessary to take advantage of the diverse views onto the data.

Concerning the analysis tasks, we figured out that almost all participants used the color mapping within the network to obtain an overview about the network attributes and particularly to identify local hubs (Analysis Task 2), where only half of them used animation to obtain an overview about the change of attributes (Analysis Task 4). To gain further insight into the data, they preferred to use "external views" to process Analysis Tasks 1, 3, and 5. When doing so, almost all of them took great advantage of the brushing and linking between the views to allocate elements.

In the future, we want to extend the tool to support the comparison of different sampling runs by loading several sets of samples for parameters, fluxes, and concentrations for the same network structure. The reactions of the networks we have analyzed so far were all based on simple kinetics. More complex kinetic equations involve up to three reaction rate coefficients and hence parameters per reaction. It should therefore be possible to visualize up to three parameters per edge, e.g., by splitting the edge into subelements. Furthermore, the measured quantities (outputs) used for parameters estimation (see Section 2.3) should be integrated and visualized within the system, e.g., using lineplots.

REFERENCES

[1] Java Universal Network/Graph Framework `http://jung.sourceforge.net/`, Nov. 2008.

[2] JMathPlot: interactive 2D and 3D plots `http://jmathtools.berlios.de/doku.php`, July 2009.

[3] Colorbrewer `http://colorbrewer2.org/`, May 2011.

[4] The Systems Biology Markup Language `http://sbml.org/`, Jan. 2012.

[5] A. Barsky, T. Munzner, J. Gardy, and R. Kincaid. Cerebral: Visualizing multiple experimental conditions on a graph with biological context. *IEEE Transactions on Visualization and Computer Graphics*, 14:1253–1260, 2008.

[6] M. Beaudouin-Lafon and W. Mackay. *Prototyping tools and techniques*, chapter The Development Process – Design and Development, pages 1017–1039. CRC, 2008.

[7] F. Beck, M. Burch, and S. Diehl. Towards an aesthetic dimensions framework for dynamic graph visualisations. In *Proceedings of 13th International Conference Information Visualization*, pages 592–597. IEEE, 2009.

[8] C. Brännmark, R. Palmer, S. T. Glad, G. Cedersund, and P. Strålfors. Mass and information feedbacks through receptor endocytosis govern insulin signaling as revealed using a parameter-free modeling framework. *Journal of Biological Chemistry*, 285(26):20171–20179, 2010.

[9] N. Cesario, A. Pang, and L. Singh. Visualizing node attribute uncertainty in graphs. In *Proceedings of the SPIE (Visualization and Data Analysis 2011)*, 2011.

[10] C. Collins, S. Carpendale, and G. Penn. Visualizing uncertainty in lattices to support decision-making. In *Proceedings of Eurographics/IEEE VGTC Symposium on Visualization*, pages 51–58. Eurographics Association, 2007.

[11] J. S. Dumas and J. E. Fox. *Usability Testing: Current Practice and Future Directions*, chapter The Development Process – Testing and Evaluation, pages 1129–1149. CRC, 2008.

[12] A. Funahashi, Y. Matsuoka, A. Jouraku, M. Morohashi, N. Kikuchi, and H. Kitano. CellDesigner 3.5: A versatile modeling tool for biochemical networks. *Proceedings of the IEEE*, 96(8):1254–1265, 2008.

[13] H. Griethe and H. Schumann. The visualization of uncertain data: Methods and problems. In *Proceedings of SimVis '06*, pages 143–156. SCS Publishing House e.V., 2006.

[14] S. Hoops, S. Sahle, R. Gauges, C. Lee, J. Pahle, N. Simus, M. Singhal, L. Xu, P. Mendes, and U. Kummer. COPASI – a COmplex PAthway SImulator. *Bioinformatics*, 22:3067–3074, 2006.

[15] M. L. Huang. Graph visualization of Web data with domain-specific attributes. In *Proceedings of the 16th International Parallel and Distributed Processing Symposium*, IPDPS '02, pages 168–174. IEEE Computer Society, 2002.

[16] C. R. Johnson. Top scientific visualization research problems. *IEEE Computer Graphics and Applications: Visualization Viewpoints*, 24(4):13–17, 2004.

[17] C. R. Johnson and A. R. Sanderson. A next step: Visualizing errors and uncertainty. *IEEE Computer Graphics and Applications*, 23(5):6–10, 2003.

[18] B. Junker, C. Klukas, and F. Schreiber. VANTED: A system for advanced data analysis and visualization in the context of biological networks. *BMC Bioinformatics*, 7(1):109–121, 2006.

[19] P. D. Karp, S. Paley, and P. Romero. The Pathway Tools software. *Bioinformatics*, 18(suppl 1):225–232, 2002.

[20] E. Klipp, R. Herwig, A. Kowald, C. Wierling, and H. Lehrach. *Systems Biology in Practice*. Wiley-VCH, Weinheim, 2005.

[21] A. Kramer, J. Hasenauer, F. Allgöwer, and N. Radde. Computation of the posterior entropy in a Bayesian framework for parameter estimation in biological networks. In *Proceedings of IEEE Multi-Conference on Systems and Control (MCS)*, pages 493–498, 2010.

[22] H. Lam, E. Bertini, P. Isenberg, C. Plaisant, and S. Carpendale. Empirical studies in information visualization: Seven scenarios. *IEEE Transactions on Visualization and Computer Graphics*, 18(9):1520–1536, 2012.

[23] B. Lee, G. G. Robertson, M. Czerwinski, and C. Sims Parr. Candidtree: visualizing structural uncertainty in similar hierarchies. *Information Visualization*, 6(3):233–246, 2007.

[24] C. Lewis. Using the "thinking-aloud" method in cognitive interface design. Technical report, IBM T. J. Watson Research Center, Yorktown Heights, NY, 1982.

[25] D. J. C. MacKay. *Information Theory, Inference, and Learning Algorithms*. Cambridge University Press, Cambridge, 7.2 edition, 2005.

[26] A. McNaught and A. Wilkinson. *IUPAC Compendium of Chemical Terminology*. Blackwell Science, 2nd edition, 1997.

[27] M. Meyer, B. Wong, M. Styczynski, T. Munzner, and H. Pfister. Pathline: A tool for comparative functional genomics. *Computer Graphics Forum*, 29(3):1043–1052, 2010.

[28] A. T. Pang, C. M. Wittenbrink, and S. K. Lodha. Approaches to uncertainty visualization. *The Visual Computer*, 13(8):370–390, 1997.

[29] A. Perer and B. Shneiderman. Integrating statistics and visualization for exploratory power: From long-term case studies to design guidelines. *IEEE Computer Graphics and Applications*, 29(3):39–51, 2009.

[30] B. Schöberl et al. Therapeutically targeting ErbB3: A key node in ligand-induced activation of the ErbB receptor–PI3K axis. *Science Signaling*, 2(77):ra31, 2009.

[31] E. R. Tufte. *Envisioning Information*. Graphics Press, Cheshire, CT, 1990.

[32] B. Tversky, J. Bauer Morrison, and M. Betrancourt. Animation: can it facilitate? *International Journal of Human-Computer Studies*, 57(4):247–262, 2002.

[33] T. von Landesberger, A. Kuijper, T. Schreck, J. Kohlhammer, J. van Wijk, J.-D. Fekete, and D. Fellner. Visual analysis of large graphs: State-of-the-art and future research challenges. *Computer Graphics Forum*, 30(6):1719–1749, 2011.

[34] C. Ware and J. C. Beatty. Using color dimensions to display data dimensions. *Human Factors*, 30(2):127–142, 1988.

[35] M. A. Westenberg, S. A. F. T. van Hijum, O. P. Kuipers, and J. B. T. M. Roerdink. Visualizing genome expression and regulatory network dynamics in genomic and metabolic context. *Computer Graphics Forum*, 27(3):887–894, 2008.

[36] D. J. Wilkinson. Bayesian methods in bioinformatics and computational systems biology. *Briefings in Bioinformatics*, 8(2):109–116, 2007.

[37] D. J. Wilkinson. Parameter inference for stochastic kinetic models of bacterial gene regulation: A Bayesian approach to systems biology. In *Proceedings of 9th Valencia International Meeting on Bayesian Statistics*, pages 679–705. Oxford University Press, 2010.